

Multiple Intersection Exponents for Planar Brownian Motion

Achim Klenke · Peter Mörters

Received: 30 November 2008 / Accepted: 24 June 2009 / Published online: 10 July 2009
© Springer Science+Business Media, LLC 2009

Abstract Let $p \geq 2$, $n_1 \leq \dots \leq n_p$ be positive integers and $B_1^1, \dots, B_{n_1}^1; \dots; B_1^p, \dots, B_{n_p}^p$ be independent planar Brownian motions started uniformly on the boundary of the unit circle. We define a p -fold intersection exponent $\varsigma_p(n_1, \dots, n_p)$, as the exponential rate of decay of the probability that the packets $\bigcup_{j=1}^{n_i} B_j^i [0, t^2]$, $i = 1, \dots, p$, have no joint intersection. The case $p = 2$ is well-known and, following two decades of numerical and mathematical activity, Lawler et al. (Acta Math. 187:275–308, 2001) rigorously identified precise values for these exponents. The exponents have not been investigated so far for $p > 2$. We present an extensive mathematical and numerical study, leading to an exact formula in the case $n_1 = 1, n_2 = 2$, and several interesting conjectures for other cases.

Keywords Brownian motion · Intersection exponent

1 Introduction

1.1 Motivation and Overview

Finding *exponents*, which describe the decay of some probabilities, and *dimensions* of some sets associated with stochastic models of physical systems is one of the core activities in statistical physics. While in general one often has to resort to numerical methods to get a handle on the values of the exponents, for planar models conformal invariance may help to answer these questions explicitly, and there is now a substantial body of rigorous and non-rigorous

A. Klenke (✉)

Institut für Mathematik, Johannes Gutenberg-Universität Mainz, Staudingerweg 9, 55099 Mainz,
Germany

e-mail: math@aklenke.de

url: <http://www.aklenke.de>

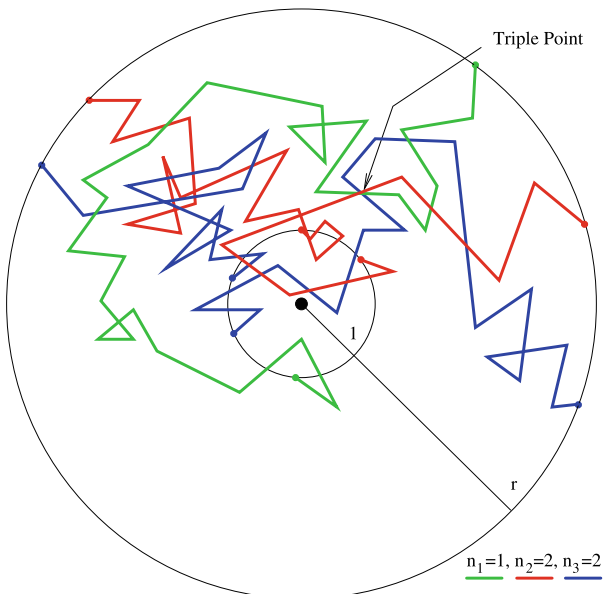
P. Mörters

Department of Mathematical Sciences, University of Bath, Claverton Down, Bath BA2 7AY, UK

e-mail: maspm@bath.ac.uk

url: <http://www.bath.ac.uk/~maspm>

Fig. 1 Illustration of a triple point ($p = 3$) with $n_1 = 1$, $n_2 = 2$ and $n_3 = 2$



methods available. For example, by making the assumption that critical planar percolation behaves in a conformally invariant way in the scaling limit and using ideas involving conformal field theory, Cardy [4] determined the asymptotic probability, as $N \rightarrow \infty$, that there exists a two-dimensional critical percolation cluster crossing a rectangle. A rigorous proof of Cardy's formula was later given by Smirnov [25]. Following considerable numerical work, see for example [18, 26] and references therein, Saleur and Duplantier [24] predicted the fractal dimension of the hull of a large percolation cluster using a non-rigorous Coulomb gas technique. Rigorous versions of this result have been given based on Cardy's formula, for example by Camia and Newman [2, 3].

In [6] Duplantier and Kwon suggested that ideas of conformal field theory can also be used to predict the probability of pairwise non-intersection between planar Brownian paths. Early research by Burdzy, Lawler and Polaski [1] and Li and Sokal [20] was of numerical nature, but ten years later, Duplantier [5] gave a derivation based on non-rigorous methods of quantum gravity, and soon after that Lawler, Schramm and Werner [14–16] gave a rigorous proof based on the Schramm-Loewner evolution (SLE), one of the greatest achievements in probability in recent years. We also mention here some very recent developments with the long term aim of making the quantum gravity approach rigorous, see Duplantier and Sheffield [7], and Rhodes and Vargas [23].

In this paper we look at joint intersections of three or more planar Brownian paths, a question which has been neglected so far in the literature, but which came up in our recent investigation of the multifractality of intersection local times [8]. In the simplest case, given three independent Brownian paths B^1, B^2, B^3 started uniformly on the unit circle, we are interested in the asymptotic behaviour, as $t \rightarrow \infty$, of the non-intersection probability

$$\mathbb{P}\{B^1[0, t] \cap B^2[0, t] \cap B^3[0, t] = \emptyset\}.$$

Observe that this probability goes to zero, for $t \uparrow \infty$, as three, or any finite number, of Brownian paths in the plane eventually intersect, see e.g. [21, Chap. 9.1]. Recall for com-

parison, that the non-intersection exponents for three Brownian paths studied in the aforementioned papers deal with pairwise non-intersections, i.e. in the case of three Brownian motions either with

$$\mathbb{P}\{B^1[0, t] \cap B^2[0, t] = \emptyset, B^2[0, t] \cap B^3[0, t] = \emptyset, B^1[0, t] \cap B^3[0, t] = \emptyset\}, \quad \text{or with}$$

$$\mathbb{P}\{B^1[0, t] \cap (B^2[0, t] \cup B^3[0, t]) = \emptyset\}.$$

Our study starts with the observation that, for positive integers n_1, \dots, n_p and independent planar Brownian motions

$$B_1^1, \dots, B_{n_1}^1; \dots; B_1^p, \dots, B_{n_p}^p,$$

nontrivial exponents

$$\varsigma_p(n_1, \dots, n_p) = -\lim_{t \rightarrow \infty} \frac{2}{\log t} \log \mathbb{P}\left\{\bigcup_{j=1}^{n_1} B_j^1[0, t] \cap \dots \cap \bigcup_{j=1}^{n_p} B_j^p[0, t] = \emptyset\right\}$$

exist, see Theorem 1 and the subsequent remark. In Theorem 2 we show that, for $2 \leq n_3 \leq \dots \leq n_p$, we have

$$\varsigma_p(1, 2, n_3, \dots, n_p) = 2.$$

These are the only exponents we could determine exactly beyond the well-known case of $p = 2$. Rigorous proofs of both theorems are given in Sect. 2.

The bulk of this paper is devoted to the presentation of a detailed numerical study of the values of the, in our opinion, most interesting remaining exponents, see Sect. 3. One of the motivations of this study was to test the conjecture, motivated by Theorem 2, that the value of the exponents $\varsigma_p(n_1, n_2, n_3, \dots, n_p)$ depend only on the two smallest parameters. This conjecture was not supported by our numerical investigations.

Finally, we remark that we have not been able to use either SLE techniques or quantum gravity to derive even a non-rigorous exact prediction of the exponents if $p > 2$. We hope however that our numerical study triggers interest in this problem and that, as in the motivational examples discussed above, future research will address the question of exact formulas for multiple intersection exponents.

1.2 Statement of the Main Theorems

Let $p \geq 2$ and n_1, \dots, n_p be positive integers and $B_1^1, \dots, B_{n_1}^1; \dots; B_1^p, \dots, B_{n_p}^p$ independent planar Brownian motions started uniformly on the unit circle $\partial\mathcal{B}(0, 1)$. We define p packets by

$$\mathfrak{B}^1(r) := \bigcup_{j=1}^{n_1} B_j^1[0, \tau_j^1(r)], \dots, \mathfrak{B}^p(r) := \bigcup_{j=1}^{n_p} B_j^p[0, \tau_j^p(r)],$$

where $\tau_j^i(r) := \inf\{t \geq 0 : |B_j^i(t)| = r\}$ and $r \geq 1$.

Theorem 1 *The limit*

$$\varsigma_p(n_1, \dots, n_p) := -\lim_{r \rightarrow \infty} \frac{1}{-\log r} \log \mathbb{P}\{\mathfrak{B}^1(r) \cap \dots \cap \mathfrak{B}^p(r) = \emptyset\}$$

exists and is positive and finite.

Remarks:

- Using a standard argument, see [13, Lemma 3.14], one can replace the paths stopped upon hitting the circle of radius r , by paths running for $t = r^2$ time units. This leads to the characterisation of the exponents given in the overview.
- For $p = 2$ all exponents are known, see [14–16]:

$$\varsigma_2(n_1, n_2) = \frac{(\sqrt{24n_1 + 1} + \sqrt{24n_2 + 1} - 2)^2 - 4}{48}.$$

The technique used to identify the exponents, which is based on the Schramm-Loewner evolution (SLE), does not seem to allow us to identify the exponents for $p > 2$.

- We conjecture that one can strengthen this result, as this was done for $p = 2$ in [12], and show that there exists a constant $c > 0$, depending on the starting points, such that

$$\lim_{r \rightarrow \infty} r^{\varsigma_p(n_1, \dots, n_p)} \mathbb{P}\{\mathfrak{B}^1(r) \cap \dots \cap \mathfrak{B}^p(r) = \emptyset\} = c.$$

However, this is quite subtle and would go beyond the scope of this paper.

There is a trivial symmetry of the exponents, namely for every permutation $\sigma \in \text{Sym}(p)$, we have

$$\varsigma_p(n_1, \dots, n_p) = \varsigma_p(n_{\sigma(1)}, \dots, n_{\sigma(p)}).$$

Moreover, there are two trivial monotonicity rules for these exponents

- (A) $\varsigma_p(n_1, \dots, n_p) \leq \varsigma_{p-1}(n_1, \dots, n_{p-1})$,
- (B) $\varsigma_p(n_1, \dots, n_p) \leq \varsigma_p(m_1, \dots, m_p)$, if $n_i \leq m_i$ for $i = 1, \dots, p$.

As a result of the symmetry of the exponents, we may henceforth assume that the arguments of the exponents are increasing in size, i.e. $n_1 \leq \dots \leq n_p$. There is one interesting situation in which we can determine the exponents explicitly.

Theorem 2 *We have $\varsigma_p(1, 2, n_3, \dots, n_p) = 2$ for any $p \geq 2$ and $2 \leq n_3 \leq \dots \leq n_p$.*

As $\varsigma_p(1, 2, \dots, 2) \leq \varsigma_p(1, 2, n_3, \dots, n_p) \leq \varsigma_2(1, 2)$ by the monotonicity rules, it suffices to show that

$$\varsigma_p(1, 2, \dots, 2) = 2. \quad (1.1)$$

The proof of this fact is based on the technique of hitting the intersection of $p - 1$ Brownian paths by a further path, using an idea of Lawler, see [10] or [11, Sect. 3], originally used to determine the exponent $\varsigma_2(1, 2) = 2$.

Remark The definition of the exponents $\varsigma_p(n_1, \dots, n_p)$ can be naturally extended to a *real* argument $\lambda > 0$ in place of n_p by letting

$$\begin{aligned} \varsigma_p(n_1, \dots, n_{p-1}, \lambda) \\ := - \lim_{r \rightarrow \infty} \frac{1}{-\log r} \log \mathbb{E} \left[\mathbb{P}\{\mathfrak{B}^1(r) \cap \dots \cap \mathfrak{B}^{p-1}(r) \cap B_1^p[0, \tau_1^p(r)] = \emptyset \right. \\ \left. | \mathfrak{B}^1(r), \dots, \mathfrak{B}^{p-1}(r)\}^\lambda \right]. \end{aligned}$$

The mapping $\lambda \mapsto \varsigma_p(n_1, \dots, n_{p-1}, \lambda)$ cannot always be analytic: for instance, recall that $\varsigma_3(1, 2, 1) \leq \varsigma_2(1, 1) = \frac{5}{4}$, but $\varsigma_3(1, 2, \lambda) = 2$ for all $\lambda \geq 2$, by Theorem 2 and the monotonicity rules. However, for $p = 2$ this mapping is analytic, see [17].

1.3 Conjectures

In this section we formulate the main conjecture motivated by our numerical studies. A detailed description of these studies and their outcomes will be given in Sect. 3.

Let $p \in \mathbb{N}$ and $n_1, \dots, n_p \in \mathbb{N}$ with $n_1 \leq n_2 \leq \dots \leq n_p$. Define

$$k := \max\{2, \min\{\ell \in \{1, \dots, p\} : n_{\ell+1} > n_\ell\}\},$$

with $k := p$ if the set is empty. We conjecture that

$$\varsigma_p(n_1, \dots, n_p) = \varsigma_k(n_1, \dots, n_k). \quad (1.2)$$

In fact, this holds, by Theorem 2 for the case $k = 2$, $n_k = 2$, and we have numerical evidence for

- $\varsigma_3(1, 1, 2) = 1.2503 \pm 0.0011$ to be compared with $\varsigma_2(1, 1) = \frac{5}{4}$
- $\varsigma_4(1, 1, 1, 2) = 1.02 \pm 0.004$ to be compared with $\varsigma_3(1, 1, 1) = 1.027 \pm 0.005$
- $\varsigma_3(2, 2, 3) = 2.937 \pm 0.01$ to be compared with $\varsigma_2(2, 2) = \frac{35}{12} = 2.91666\dots$

This is evidence that if p packets of Brownian motions are required not to intersect, this is achieved by the k smallest packets not intersecting, if these are *strictly* smaller than the $p - k$ largest packets. Beyond this conjecture it is interesting to compare further values, namely

- $\varsigma_3(1, 3, 3) = 2.688 \pm 0.01$ with $\varsigma_2(1, 3) = \frac{13+\sqrt{73}}{8} = 2.693000\dots$
- $\varsigma_3(2, 3, 3) = 3.767 \pm 0.06$ with $\varsigma_2(2, 3) = \frac{47+5\sqrt{73}}{24} = 3.738334113\dots$,

which is evidence supporting the conjecture that in some cases nonintersection is achieved by the two smallest packets not intersecting, even if the second and third smallest have the same size. However this cannot be expected in all situations, as can be seen comparing

- $\varsigma_3(1, 1, 1) = 1.027 \pm 0.005$ with $\varsigma_2(1, 1) = \frac{5}{4}$.

2 Proofs of Theorems 1 and 2

2.1 Proof of Theorem 1

Denote by $x = (x_1^1, \dots, x_{n_1}^1; \dots; x_1^p, \dots, x_{n_p}^p)$ vectors with $n_1 + \dots + n_p$ entries in \mathbb{R}^2 , playing the role of configurations of our motions at time zero. Consider

$$a_r := \sup_{|x_j^i|=1} \mathbb{P}_x \{ \mathfrak{B}^1(r) \cap \dots \cap \mathfrak{B}^p(r) = \emptyset \},$$

where the subindex of \mathbb{P} indicates the starting points of the Brownian motions. Using the strong Markov property and Brownian scaling, we get, for any $r, s \geq 1$,

$$\begin{aligned} a_{rs} &\leq \sup_{|x_j^i|=1} \mathbb{P}_x \left\{ \bigcup_{j=1}^{n_1} B_j^1[0, \tau_j^1(r)] \cap \cdots \cap \bigcup_{j=1}^{n_p} B_j^p[0, \tau_j^p(r)] = \emptyset, \right. \\ &\quad \left. \bigcup_{j=1}^{n_1} B_j^1[\tau_j^1(r), \tau_j^1(rs)] \cap \cdots \cap \bigcup_{j=1}^{n_p} B_j^p[\tau_j^p(r), \tau_j^p(rs)] = \emptyset \right\} \\ &= \sup_{|x_j^i|=1} \mathbb{E}_x \left[1 \left\{ \bigcup_{j=1}^{n_1} B_j^1[0, \tau_j^1(r)] \cap \cdots \cap \bigcup_{j=1}^{n_p} B_j^p[0, \tau_j^p(r)] = \emptyset \right\} \right. \\ &\quad \times \mathbb{P}_{(B_j^i(\tau_j^i(r)))} \left. \left\{ \bigcup_{j=1}^{n_1} B_j^1[\tau_j^1(r), \tau_j^1(rs)] \cap \cdots \cap \bigcup_{j=1}^{n_p} B_j^p[\tau_j^p(r), \tau_j^p(rs)] = \emptyset \right\} \right] \\ &\leq a_r a_s. \end{aligned}$$

Hence the function given by $b_t := \log a_{2^t}$ is subadditive and, by the subadditivity lemma, see e.g. [11, Lemma 5.2.1], we thus have $\lim_{t \rightarrow \infty} b_t/t = \inf_{t>0} b_t/t$. Therefore,

$$\tilde{s}_p(n_1, \dots, n_p) := - \lim_{r \rightarrow \infty} \frac{1}{\log r} \log \sup_{|x_j^i|=1} \mathbb{P}_x \{ \mathfrak{B}^1(r) \cap \cdots \cap \mathfrak{B}^p(r) = \emptyset \}$$

exists, and is positive.

Next, we show that we can replace the optimised starting points by starting points uniformly chosen from the unit circle. Clearly, we have

$$\mathbb{P} \{ \mathfrak{B}^1(r) \cap \cdots \cap \mathfrak{B}^p(r) = \emptyset \} \leq \sup_{|x_j^i|=1} \mathbb{P}_x \{ \mathfrak{B}^1(r) \cap \cdots \cap \mathfrak{B}^p(r) = \emptyset \}, \quad (2.1)$$

where \mathbb{P} refers to the original scenario of Brownian motions started uniformly on the unit circle.

Conversely, using the Markov property, for $r > 2$, we have

$$\begin{aligned} &\sup_{|x_j^i|=1} \mathbb{P}_x \{ \mathfrak{B}^1(r) \cap \cdots \cap \mathfrak{B}^p(r) = \emptyset \} \\ &\leq \sup_{|x_j^i|=1} \mathbb{E}_x \left[\mathbb{P}_{(B_j^i(\tau_j^i(2)))} \left\{ \bigcup_{j=1}^{n_1} B_j^1[\tau_j^1(2), \tau_j^1(r)] \cap \cdots \cap \bigcup_{j=1}^{n_p} B_j^p[\tau_j^p(2), \tau_j^p(r)] = \emptyset \right\} \right]. \end{aligned}$$

By the Harnack principle, the law of the vector $(B_j^i(\tau_j^i(2)))$ is bounded, uniformly in x , by a constant multiple of the uniform distribution on the $(n_1 + \cdots + n_p)$ -fold Cartesian power of the circle $\partial\mathcal{B}(0, 2)$. Denoting this constant by C and using Brownian scaling,

$$\begin{aligned} &\mathbb{P} \left\{ \bigcup_{j=1}^{n_1} B_j^1[0, \tau_j^1(r/2)] \cap \cdots \cap \bigcup_{j=1}^{n_p} B_j^p[0, \tau_j^p(r/2)] = \emptyset \right\} \\ &\geq C^{-1} \sup_{|x_j^i|=1} \mathbb{P}_x \{ \mathfrak{B}^1(r) \cap \cdots \cap \mathfrak{B}^p(r) = \emptyset \}. \end{aligned} \quad (2.2)$$

Combining (2.1) and (2.2) yields that

$$\varsigma_p(n_1, \dots, n_p) := -\lim_{r \rightarrow \infty} \frac{1}{\log r} \log \mathbb{P}\{\mathfrak{B}^1(r) \cap \dots \cap \mathfrak{B}^p(r) = \emptyset\}$$

exists and coincides with $\tilde{\varsigma}_p(n_1, \dots, n_p)$. Note, finally, that the monotonicity rule (A) implies that $\varsigma_p(n_1, \dots, n_p) \leq \varsigma_2(n_1, n_2) < \infty$, and hence the exponents are positive and finite.

2.2 Proof of Theorem 2

Recall that it suffices to show (1.1). We start by formulating the key lemma. We let W^1, \dots, W^p be independent Brownian paths. For $r, s > 0$ denote by $\tau^i(x, r)$ the first hitting time by the motion W^i of the circle $\partial\mathcal{B}(x, r)$ with centre x and radius r , and let $\tau^i(x, r, s)$ be the first hitting time of $\partial\mathcal{B}(x, s)$ after $\tau^i(x, r)$.

Lemma 3 Fix $x \in \mathcal{B}(0, 1)$. Suppose that W^1, \dots, W^p are independent Brownian paths started uniformly on the circle $\partial\mathcal{B}(0, 2)$. Define the set

$$\mathfrak{W} := \bigcap_{j=2}^p W^j[0, \tau^j(0, 4)] \quad (2.3)$$

and the events

$$\begin{aligned} E_{x,r} &= \{W^1[0, \tau^1(x, r/2)] \cap \mathfrak{W} = \emptyset\}, \\ N_{x,r} &= \{W^1[0, \tau^1(x, r/2, r)] \cap \mathfrak{W} \neq \emptyset\}, \\ H_{x,r} &= \{\tau^i(x, r/2) < \tau^i(0, 4) \text{ for all } i = 1, \dots, p\}. \end{aligned} \quad (2.4)$$

Then

$$\liminf_{r \downarrow 0} \frac{1}{|\log r|} \log \mathbb{P}[E_{x,r} \cap N_{x,r} | H_{x,r}] \geq -\varsigma_p(1, 2, \dots, 2).$$

Let us first see how (1.1) follows from this lemma. Let

$$\tau = \inf\{t > 0 : W^1(t) \in \mathfrak{W}\}.$$

Now let \mathfrak{B} be a collection of pairwise disjoint discs of fixed radius $0 < r < 1/2$ with centres in the disc $\mathcal{B}(0, 1)$, which has cardinality at least $(2r)^{-2}$. Then, obviously,

$$1 \geq \mathbb{P}\{W^1[0, \tau^1(0, 4)] \cap \mathfrak{W} \neq \emptyset\} \geq \sum_{\mathcal{B} \in \mathfrak{B}} \mathbb{P}\{W^1(\tau) \in \mathcal{B}, \tau < \tau^1(0, 4)\}.$$

Now, fix a disc $\mathcal{B} = \mathcal{B}(x, r) \in \mathfrak{B}$. The event $\{W^1(\tau) \in \mathcal{B}, \tau < \tau^1(0, 4)\}$ is implied by the events

$$E_{x,r} \cap N_{x,r} \cap \{\tau^1(x, r/2) < \tau^1(0, 4)\}.$$

Recall that

$$\mathbb{P}[H_{x,r}] = \mathbb{P}\{\tau^1(x, r/2) < \tau^1(0, 4)\}^p = r^{o(1)}.$$

Combining this with Lemma 3, for any $\varepsilon > 0$ and sufficiently small $r > 0$,

$$\mathbb{P}\{W^1(\tau) \in \mathcal{B}, \tau < \tau^1(0, 4)\} \geq r^{\varsigma_p(1, 2, \dots, 2) + \varepsilon}.$$

This implies

$$1 \geq \sum_{B \in \mathfrak{B}} r^{\varsigma_p(1, 2, \dots, 2) + \varepsilon} \geq r^{-2 + \varsigma_p(1, 2, \dots, 2) + 2\varepsilon},$$

and therefore $\varsigma_p(1, 2, \dots, 2) \geq 2 - 2\varepsilon$. The lower bound follows as $\varepsilon > 0$ was arbitrary, and the upper bound in (1.1) follows from $\varsigma_p(1, 2, \dots, 2) \leq \varsigma_2(1, 2) = 2$, as is known from [10, 11].

Proof of Lemma 3 Before we describe the technical details we sketch the idea of the proof. Since the paths of p planar Brownian motions intersect with positive probability, by Brownian scaling, the conditional probability of $N_{x,r}$ given $H_{x,r}$ is bounded from below as $r \rightarrow 0$. Hence this condition can be neglected when computing the probability in Lemma 3. For $j = 1, \dots, p$ we decompose the paths W^j into the pieces $W^j[0, \tau^j(x, r/2)]$ and $W^j[\tau^j(x, r/2), \tau^j(0, 4)]$. By time reversal for $W^j[0, \tau^j(x, r/2)]$, we can compare the probability in question with the non-intersection probability for packets of size $n_1 = 1$, $n_2 = \dots = n_p = 2$, which is of order $\approx r^{\varsigma_p(1, 2, \dots, 2)}$.

We now come to the technical details, see the appendix in [22] for the necessary facts about Brownian excursions between concentric spheres. Let $\varrho^1 = r$ and $\varrho^j = r/2$ for $j = 2, \dots, p$. Conditioned on $\{\tau^i(x, \varrho^j/2) < \tau^i(x, 3)\}$ the path $W^i[0, \tau^i(x, \varrho^j/2)]$ is contained in an excursion from $\partial\mathcal{B}(x, 3)$ to $\partial\mathcal{B}(x, \varrho^j/2)$. The time-reversal of this excursion is contained in the path of a Brownian motion \tilde{W}^i started uniformly on $\partial\mathcal{B}(x, \varrho^j/2)$ and stopped upon reaching $\partial\mathcal{B}(x, 3)$, say at time $\tilde{\tau}^i(x, 3)$. Analogously to (2.3) and (2.4) define the set

$$\tilde{\mathfrak{W}} = \bigcap_{j=2}^p (\tilde{W}^j[0, \tilde{\tau}^j(x, 3)] \cup W^j[\tau^j(x, r/4, r/2), \tau^j(0, 4)]),$$

and the events

$$\begin{aligned} \tilde{E}_{x,r} &= \{\tilde{W}^1[0, \tilde{\tau}^1(x, 3)] \cap \tilde{\mathfrak{W}} = \emptyset\}, \\ \tilde{N}_{x,r} &= \left\{ \bigcap_{j=1}^p W^j[\tau^j(x, \varrho^j/2), \tau^j(x, \varrho^j/2, \varrho^j)] \neq \emptyset \right\}, \\ \tilde{H}_{x,r} &= \{\tau^j(x, \varrho^j/2) < \tau^j(x, 3) \text{ for all } j = 1, \dots, p\}. \end{aligned}$$

Note that $W^1[0, \tau^1(x, \varrho^1)] \cap \mathcal{B}(x, r/2) = \emptyset$ and $W^j[\tau^j(x, \varrho^j/2), \tau^j(x, \varrho^j/2, \varrho^j)] \subset \mathcal{B}(x, r/2)$ for $j = 2, \dots, p$. Hence

$$W^1[0, \tau^1(x, \varrho^1)] \cap (\mathfrak{W} \setminus \tilde{\mathfrak{W}}) \subset W^1[0, \tau^1(x, \varrho^1)] \cap \bigcap_{j=2}^p W^j[\tau^j(x, \varrho^j/2), \tau^j(x, \varrho^j/2, \varrho^j)] = \emptyset$$

which implies $\tilde{E}_{x,r} \subset E_{x,r}$. Note that trivially, we have $\tilde{H}_{x,r} \subset H_{x,r}$ and $\tilde{N}_{x,r} \subset N_{x,r}$ which implies

$$E_{x,r} \cap N_{x,r} \cap H_{x,r} \supset \tilde{E}_{x,r} \cap \tilde{N}_{x,r} \cap \tilde{H}_{x,r}. \quad (2.5)$$

Finally, note that

$$f(x, r) := \frac{\mathbb{P}[\tilde{H}_{x,r}]}{\mathbb{P}[H_{x,r}]} = \frac{\mathbb{P}\{\tau^1(x, \varrho^1/2) < \tau^1(x, 3)\}^p}{\mathbb{P}\{\tau^1(x, r/2) < \tau^1(0, 4)\}^p} \geq \frac{1}{2} \quad (2.6)$$

for all x and for sufficiently small values of $r > 0$.

By (2.5), (2.6) and the definition of the conditional probability, we conclude

$$\mathbb{P}[E_{x,r} \cap N_{x,r} | H_{x,r}] \geq f(x, r) \mathbb{P}[\tilde{E}_{x,r} \cap \tilde{N}_{x,r} | \tilde{H}_{x,r}]. \quad (2.7)$$

Fix $\varepsilon > 0$. Invoking the definition of the exponent, the Harnack principle and Brownian scaling, for sufficiently small $r > 0$,

$$\mathbb{P}[\tilde{E}_{x,r} | \tilde{H}_{x,r}] \geq r^{\varsigma_p(1, 2, \dots, 2) + \varepsilon}.$$

Define the compact sets

$$C := \{y = (y^1, \dots, y^p) : y^j \in \partial\mathcal{B}(0, \varrho^j/2) \text{ for } j = 1, \dots, p\} \quad \text{and}$$

$$D := \{z = (z^1, \dots, z^p) : z^j \in \partial\mathcal{B}(0, \varrho^j) \text{ for } j = 1, \dots, p\}.$$

For $y \in C$ and $z \in D$ let $(\bar{W}^j, j = 1, \dots, p)$ be an independent family of Brownian motions where each motion \bar{W}^j is started at y^j and is conditioned to leave $\mathcal{B}(0, \varrho^j)$ at z^j (at time $\bar{\tau}^j$). Denote by $\mathbb{P}_{y,z}$ the corresponding probability measure. It is easy to see that the map

$$\phi : C \times D \rightarrow [0, 1], \quad (y, z) \mapsto \mathbb{P}_{y,z}\{\bar{W}^1[0, \tau^1] \cap \dots \cap \bar{W}^p[0, \tau^p] \neq \emptyset\}$$

is continuous and strictly positive, and independent of r by Brownian scaling. Hence

$$c := \inf_{y \in C, z \in D} \phi(y, z) > 0.$$

We infer that

$$\mathbb{P}[\tilde{N}_{x,r} | \tilde{E}_{x,r} \cap \tilde{H}_{x,r}] \geq c > 0.$$

Hence, combining our results, for sufficiently small $r > 0$

$$\mathbb{P}[\tilde{E}_{x,r} \cap \tilde{N}_{x,r} | \tilde{H}_{x,r}] = \mathbb{P}[\tilde{E}_{x,r} | \tilde{H}_{x,r}] \mathbb{P}[\tilde{N}_{x,r} | \tilde{E}_{x,r} \cap \tilde{H}_{x,r}] \geq c r^{\varsigma_p(1, 2, \dots, 2) + \varepsilon},$$

and this completes the proof as $\varepsilon > 0$ was arbitrary. \square

3 Simulations

To get hold of those exponents which we could not determine explicitly, we have performed Monte Carlo simulations. This has successfully generated conjectures in the $p = 2$ case, see Duplantier and Kwon [6], Li and Sokal [20] and Burdzy, Lawler and Polaski [1].

3.1 The General Scheme

Before we list and analyse the simulated data, we explain how we got it. Fix positive integers p and n_1, \dots, n_p . The aim is to get an estimate on $\varsigma_p(n_1, \dots, n_p)$. Instead of Brownian motions we simulate two-dimensional symmetric nearest neighbour random walks. As it reduces computing effort, we work with boxes rather than with discs. (For comparison we have performed some of the simulations also with discs and there was no significant difference in the results.) First we fix an increasing sequence of box half-lengths L_0, \dots, L_K (in most cases $L_{k+1} = \lfloor 1.1 \cdot L_k \rfloor$ and the maximal value $m = L_L$ restricted to 20 000, 40 000 or 80 000) and the sample size N of the simulation.

Step 1. We start $n_1 + \dots + n_p$ independent random walks at the origin $0 \in \mathbb{Z}^2$ and stop each of them when it hits the (graph) boundary of the box $\{-L_0, \dots, L_0\}^2 = [-L_0, L_0]^2 \cap \mathbb{Z}^2$. This defines the starting positions of the random walks.

Step 2. Assume we are at level k (after Step 1 we are at level $k = 1$). Independently run the random walks until they hit the boundary of the box $\{-L_k, \dots, L_k\}^2 \subset \mathbb{Z}^2$. Separately, keep track of the set $A_{k,i} \subset \{-L_k + 1, \dots, L_k - 1\}^2$ of points that are visited by the i th package of n_i random walks *before* hitting the boundary of $\{-L_k, \dots, L_k\}^2$ (after Step 1).

If $A_{k,1} \cap \dots \cap A_{k,p} = \emptyset$, then we say that we have *survived* level k and we enter level $k + 1$ (that is, we perform Step 2 again with k replaced by $k + 1$). Otherwise we stop this sample and start a new simulation in Step 1.

By N_k we denote the number of samples that have survived level k . Clearly, $N_0 = N$. We should have

$$N_k/N \approx (L_k/L_0)^{-\varsigma_p(n_1, \dots, n_p)}.$$

Hence in a double logarithmic plot of $\log(N_k)$ against $\log(L_k)$ the points should be on a line with slope $-\varsigma_p(n_1, \dots, n_p)$. Linear regression then gives an estimate for the exponent $\varsigma_p(n_1, \dots, n_p)$.

As it turns out that a line can be fitted well only for large values of L_k , we have neglected the small values of L_k in order to get a reasonable estimate for $\varsigma_p(n_1, \dots, n_p)$. In Fig. 2 below we plotted the data points used for the linear regression with solid circles, the other points with hollow circles.

As can be seen from Fig. 2, for $\xi(1, 1)$ this gives a pretty good estimate of the exact value $\frac{5}{4}$, even with a moderate computing effort of about 2000 hours CPU time. However, for $\xi(1, 1, 1)$ the points tend to lie on a straight line only for large values of L_k and thus require

- (i) a large maximal box size $m = L_K$ and thus a big computer memory of size $(2m + 1)^2$ bytes in order to keep track of the visited points,
- (ii) a large sample size N_0 in order that $N_K \approx N_0 \cdot (L_K/L_0)^{-\xi(1, 1, 1)}$ is big enough to obtain reliable data from the simulation.

Since the CPU time we need for each sample grows with m , (i) and (ii) imply that we need huge amounts of CPU time. Furthermore, with huge sample sizes and box sizes, we run into the order of the cycle length of the common 48 bit linear congruence random number generators.

The computations were performed on different computers, mainly on two parallel Linux clusters at the University of Mainz on Opteron 2218 processors with 2.6 GHz and on Opteron 244 processors with 1.8 GHz. The programme code is written in C. As random number generator we used drand64(), a 64 bit linear congruence generator following the rule

$$r_{n+1} = (ar_n + c) \mod 2^{64}$$

with

$$a = 6364136223846793005 \quad \text{and} \quad c = 1$$

(see [9, pp. 106–108]).

The linear regression method does not give a quantitative estimate on the statistical error. In order to get such an error estimate we did the following. Having in mind that the systematic error is large for small box sizes, we choose a minimal box number $k_{\min} \in \{1, \dots, K - 1\}$

and neglect the data from all smaller boxes. Furthermore, we pretend that the asymptotics for p_L is exact for $k \geq k_{\min}$, that is,

$$p_{L_k} = CL_k^{-\zeta} \quad \text{for all } k \geq k_{\min} \quad (3.1)$$

for some $C > 0$. In particular, the conditional probability to have no multiple intersections before leaving $B_{L_{k+1}}$ given there is no multiple intersection before leaving B_{L_k} is

$$\bar{p}_k := \frac{p_{L_{k+1}}}{p_{L_k}} = \left(\frac{L_k}{L_{k+1}} \right)^{-\zeta} =: q_k^{-\zeta}.$$

Here the likelihood function for the observation

$$(N_{k_{\min}}, N_{k_{\min}+1}, \dots, N_K) = n := (n_{k_{\min}}, n_{k_{\min}+1}, \dots, n_K)$$

is

$$\begin{aligned} L_n(\zeta) &= C(n) \prod_{l=k_{\min}}^{K-1} \bar{p}_l^{n_{l+1}} (1 - \bar{p}_l)^{n_l - n_{l+1}} \\ &= C(n) \prod_{l=k_{\min}}^{K-1} \bar{q}_l^{\zeta n_{l+1}} (1 - \bar{q}_l^\zeta)^{n_l - n_{l+1}} \end{aligned} \quad (3.2)$$

for some $C(n) > 0$. The log-likelihood function is

$$\mathcal{L}_n(\zeta) = \log C(n) + \sum_{l=k_{\min}}^{K-1} (n_{l+1}\zeta \log(q_l) + (n_l - n_{l+1}) \log(1 - q_l^\zeta)). \quad (3.3)$$

The maximum likelihood estimator (MLE) $\hat{\zeta}$ is defined by

$$\mathcal{L}_n(\hat{\zeta}) = \sup_{\zeta > 0} \mathcal{L}_n(\zeta). \quad (3.4)$$

We compute the derivatives

$$\mathcal{L}'_n(\zeta) = \sum_{l=k_{\min}}^{K-1} n_{l+1} \log(q_l) - \sum_{l=k_{\min}}^{K-1} (n_l - n_{l+1}) \frac{\log(q_l) q_l^\zeta}{1 - q_l^\zeta} \quad (3.5)$$

and

$$\mathcal{L}''_n(\zeta) = - \sum_{l=k_{\min}}^{K-1} (n_l - n_{l+1}) \frac{(\log(q_l))^2 q_l^\zeta}{(1 - q_l^\zeta)^2}. \quad (3.6)$$

Clearly, $\mathcal{L}''_n(\zeta) < 0$, hence $\zeta \mapsto \mathcal{L}_n(\zeta)$ is strictly concave and thus $\hat{\zeta}$ is the unique solution of

$$\mathcal{L}'_n(\hat{\zeta}) = 0. \quad (3.7)$$

Hence, for given data, the MLE can easily be computed numerically (we used a Newton approximation scheme).

Denote by $\hat{\varsigma}_{n_0}$ the MLE for sample size n_0 . By standard theory for MLEs, $(\hat{\varsigma})_{n_0 \in \mathbb{N}}$ is consistent and asymptotically normally distributed. In fact, by Corollary 6.2.1 of [19],

$$\hat{\varsigma}_{n_0} \xrightarrow{n_0 \rightarrow \infty} \varsigma \quad \text{stochastically.} \quad (3.8)$$

Furthermore, by [19, Corollary 6.2.3], $(\hat{\varsigma})_{n_0}$ is asymptotically efficient (that is, optimal) and by [19, Theorem 6.2.3] (with $\mathcal{N}_{0,1}$ the standard normal distribution)

$$\sqrt{n_0 I(\varsigma)} (\hat{\varsigma}_{n_0} - \varsigma) \xrightarrow{n_0 \rightarrow \infty} \mathcal{N}_{0,1} \quad \text{in distribution.} \quad (3.9)$$

Here

$$I(\varsigma) = -\mathbb{E}[\mathcal{L}_N''(\varsigma) | N_0 = 1] = p_{L_{k_{\min}}} \sum_{l=k_{\min}}^{K-1} \left(\prod_{m=k_{\min}}^{l-1} \bar{p}_m \right) (1 - \bar{p}_l) \frac{(\log(q_l))^2 q_l^\varsigma}{(1 - q_l^\varsigma)^2} \quad (3.10)$$

is the Fisher information for one sample. As we do not know the true value of ς and since we do not know $p_{L_{k_{\min}}}$, we replace $I(\varsigma)$ by

$$I_n(\varsigma) = -\frac{1}{n_0} \mathcal{L}_n''(\varsigma).$$

By the law of large numbers $I_N(\varsigma) \xrightarrow{n_0 \rightarrow \infty} I(\varsigma)$ almost surely, uniformly in ς in compact sets. Hence by (3.8), we have $I_N(\hat{\varsigma}) \xrightarrow{n_0 \rightarrow \infty} I(\varsigma)$ stochastically. Hence we use

$$\hat{\sigma}^2 := -1/\mathcal{L}_N''(\hat{\varsigma}) \quad (3.11)$$

as an estimator for the variance of $\hat{\varsigma}$ and obtain

$$\frac{\hat{\varsigma} - \varsigma}{\hat{\sigma}} \xrightarrow{n_0 \rightarrow \infty} \mathcal{N}_{0,1} \quad \text{in distribution.} \quad (3.12)$$

Concluding, an asymptotic 95% confidence interval for ς is given by

$$[\hat{\varsigma} - 2\hat{\sigma}, \hat{\varsigma} + 2\hat{\sigma}]. \quad (3.13)$$

We have performed the simulations for the exponents $\varsigma_2(1, 1)$ and $\varsigma_2(2, 2)$ as benchmark problems, and then did the simulations on a larger scale for

$$\varsigma_3(1, 1, 1), \quad \varsigma_3(1, 1, 2), \quad \varsigma_4(1, 1, 1, 1), \quad \varsigma_4(1, 1, 1, 2).$$

3.2 Two-Level Scheme

The simulations turn out to be very time-consuming, especially for the exponents with a larger numerical value. In order to get a more efficient scheme in this situation consider the following simplification of the simulation scheme presented above:

Assume there are only three box sizes, L_0 (about 30), L_1 (about 10 000) and $L_2 = 2L_1$. Then (3.7) can be solved explicitly and the maximum likelihood estimator for ς is

$$\hat{\varsigma} = -\frac{\log(n_2/n_1)}{\log(2)}.$$

In order to reduce the variance of $\hat{\varsigma}$ we have to increase N_1 , that is the sample size n_0 . However, since it takes much CPU time to obtain a sample that contributes to N_1 , we may wish to use this very sample as the starting point for a number m of trials running from box size L_1 to L_2 . Assume that x among these m trials have survived until L_2 (that is, have reached the boundary of the L_2 -box without producing a multiple intersection), then $p_S = \frac{x}{m}$ is an estimator for the conditional probability of producing no multiple intersection until leaving the L_2 -box for the given realisation S of the paths of all walks in the L_1 -box. Now we can prescribe the number $n = n_1$ of “master samples” and for $i = 1, \dots, n$ let x_i be the corresponding number of surviving trials and write $\hat{p}_i := x_i/m$. Hence for

$$p := \frac{p_{L_2}}{p_{L_1}} = \mathbb{E}[p_S]$$

we get the unbiased estimator

$$\hat{p} = \frac{1}{n} \sum_{i=1}^n \hat{p}_i.$$

The unbiased estimator for the variance of \hat{p} is

$$\hat{\sigma}_p^2 = \frac{1}{n(n-1)} \sum_{i=1}^n (\hat{p}_i - \hat{p})^2.$$

From \hat{p} and $\hat{\sigma}_p^2$ we obtain the estimators for ς and the variance σ^2 of $\hat{\varsigma}$

$$\hat{\varsigma} = -\frac{\log(p)}{\log(2)} \quad \text{and} \quad \hat{\sigma}^2 = \frac{\hat{\sigma}_p^2}{(\log(2)\hat{p})^2}. \quad (3.14)$$

We have employed this scheme for the exponents with numerical values larger than 2, and we explain now why it is more efficient in these cases.

The expected time planar random walk needs to go from the boundary of $\{-L, \dots, L\}^2$ to the boundary of $\{-L-1, \dots, L+1\}^2$ is of order L . The probability that a given sample ever reaches the boundary of $\{-L-1, \dots, L+1\}^2$ is of order $L^{-\varsigma}$. Hence (if we stop the simulation as soon as the first multiple intersection is detected) the expected CPU time for each sample until box size L_1 is of order

$$\sum_{L=L_0}^{L_1} L^{1-\varsigma}.$$

For $\varsigma > 2$ this sum is of order 1, for $\varsigma \leq 2$, it is of order $L_1^{2-\varsigma}$. Now the probability that a sample reaches box size L_1 without producing a multiple intersection is of order $L_1^{-\varsigma}$. Hence the expected CPU time needed for simulating a “master sample” is of order $L_1^{2\vee\varsigma}$. On the other hand, each of the trials started from the master sample needs an expected CPU time of order L_1^2 . Hence for $\varsigma > 2$ we can run $m = L_1^{\varsigma-2}$ trials without increasing the CPU significantly.

In order to make a good choice for m , compute the variance of \hat{p}

$$\text{Var}[\hat{p}] = n^{-1}\text{Var}[p_S] + \frac{1}{mn}\mathbb{E}[p_S(1-p_S)] \leq n^{-1}\text{Var}[p_S] + \frac{1}{mn}\mathbb{E}[p_S].$$

The quantities $\text{Var}[p_S]$ and $\mathbb{E}[p_S] \approx 2^{-\zeta}$ can be estimated from a test simulation as well as the expected CPU time T_1 to produce a master sample and the expected time T_2 used for each subsequent trial. Now it is an optimisation problem for the total CPU time $n(T_1 + mT_2)$ versus the variance $\text{Var}[\hat{p}]$. For some of the simulations we have done test runs and solved the optimisation problem. Here $m = 1000$ turned out to be a reasonable choice that we have then used in all simulations.

We have performed the simulations according to this scheme with $L_0 = 30$, $L_1 = 10000$, $L_2 = 20000$ and $m = 1000$ for the exponents

$$\varsigma_3(1, 3, 3), \quad \varsigma_3(2, 2, 2), \quad \varsigma_3(2, 2, 3), \quad \varsigma_3(2, 3, 3), \quad \varsigma_4(2, 2, 2, 2).$$

3.3 Numerical Results

We present our estimated values $\hat{\zeta}$ together with a statistical error of 2σ . For the systematic error it is hard to make a good judgement. From the graphical representation of the results (see below) it seems that for $\varsigma_3(1, 1, 2)$ the systematic error is of a smaller order than the statistical error. For $\varsigma_3(1, 1, 2)$ and $\varsigma_3(1, 1, 1)$ it is presumably of the same order. Finally, for $\varsigma_4(1, 1, 1, 1)$ and, even worse for $\varsigma_5(1, 1, 1, 1, 1)$ we seem to systematically underestimate the values. It would require a lot larger L_{\max} to get more accurate results. For that reason we have not taken too much effort to reduce the statistical error. However, we give the results of the simulations just to provide an idea of the possible values.

Table 1 Numerical results obtained from the first simulation scheme

exponent	$\hat{\zeta}$	$2\hat{\sigma}$	rigorous	L_{\min}	L_{\max}	$n_0/10^6$	CPU time/h
$\varsigma_2(1, 1)$	1.2502	0.001	$5/4$	1069	20 000	500	2064
$\varsigma_2(2, 2)$	2.9188	0.0033	$\frac{35}{12} = 2.9167$	163	20 000	40 000	1879
$\varsigma_3(1, 1, 1)$	1.027	0.005	$[1/2, 5/4]$	18 575	80 000	60	8262
$\varsigma_3(1, 1, 2)$	1.2503	0.0011	$[1, 5/4]$	1069	80 000	200	5858
$\varsigma_4(1, 1, 1, 1)$	0.877	0.006	$[1/4, 5/4]$	39 813	80 000	20	18 262
$\varsigma_4(1, 1, 1, 2)$	1.02	0.004	$[1/2, 5/4]$	27 194	40 000	200	35 212
$\varsigma_5(1, 1, 1, 1, 1)$	0.74	0.02	$[1/8, 5/4]$	27 194	40 000	0.74	1147

Table 2 Numerical results obtained from the second simulation scheme

exponent	$\hat{\zeta}$	$2\hat{\sigma}$	rigorous	n	CPU time/h
$\varsigma_3(1, 3, 3)$	2.688	0.01	$[2, (13 + \sqrt{73})/8]$	18 100	61 860
$\varsigma_3(2, 2, 2)$	2.786	0.01	$[2, 35/12]$	16 000	47 943
$\varsigma_3(2, 2, 3)$	2.937	0.01	$[2, 35/12]$	23 000	116 888
$\varsigma_3(2, 3, 3)$	3.767	0.057	$[2, 35/12]$	1000	179 543
$\varsigma_4(2, 2, 2, 2)$	2.664	0.01	$[2, 35/12]$	16 000	63 496

3.4 Detailed Data

3.4.1 Exponent $\zeta_2(1, 1)$

The exact value $\zeta_2(1, 1) = 5/4$ is known. This simulation is used as a benchmark test for our simulation.

L_k	n_k	L_k	n_k	L_k	n_k	L_k	n_k	L_k	n_k
30	500 000 000	113	109 366 745	455	19 660 552	1890	3 323 382	7881	557 957
33	455 164 209	124	97 714 439	500	17 483 797	2079	2 950 258	8669	495 180
36	414 185 142	136	87 320 799	550	15 525 080	2286	2 620 862	9535	439 662
39	379 373 384	149	78 109 962	605	13 788 917	2514	2 327 160	10 488	389 839
42	349 383 901	163	69 978 568	665	12 253 892	2765	2 066 024	11 536	345 918
46	315 390 855	179	62 384 176	731	10 890 052	3041	1 834 523	12 689	307 046
50	286 840 826	196	55 800 459	804	9 669 275	3345	1 628 901	13 957	272 420
55	257 075 021	215	49 786 852	884	8 589 857	3679	1 446 024	15 352	241 798
60	232 385 705	236	44 382 636	972	7 631 215	4046	1 283 655	16 887	214 746
66	207 870 728	259	39 563 995	1069	6 776 772	4450	1 140 213	18 575	190 486
72	187 620 511	284	35 298 660	1175	6 020 939	4895	1 012 659	20 000	173 506
79	168 084 821	312	31 418 279	1292	5 347 118	5384	898 680		
86	151 902 122	343	27 932 867	1421	4 747 333	5922	797 641		
94	136 553 134	377	24 837 149	1563	4 214 131	6514	708 293		
103	122 326 905	414	22 109 889	1719	3 741 150	7165	628 813		

Values used for the fit: $L_k = 1069 \dots 20\,000$. CPU time 2064 h.

Fig. 2 Linear regression for the simulation of $\zeta_2(1, 1)$

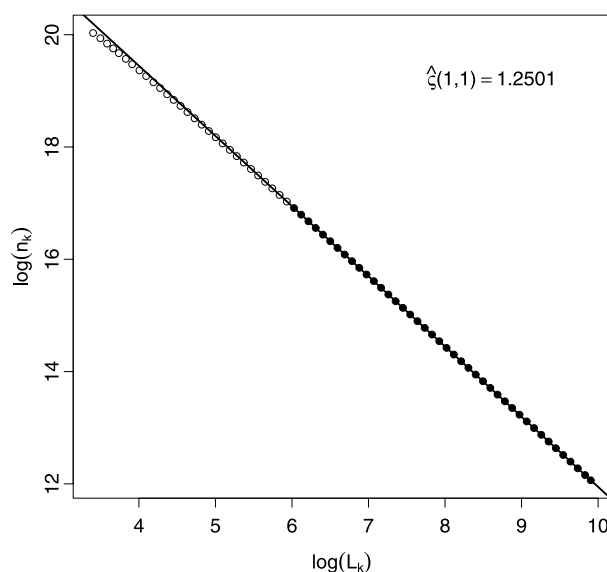
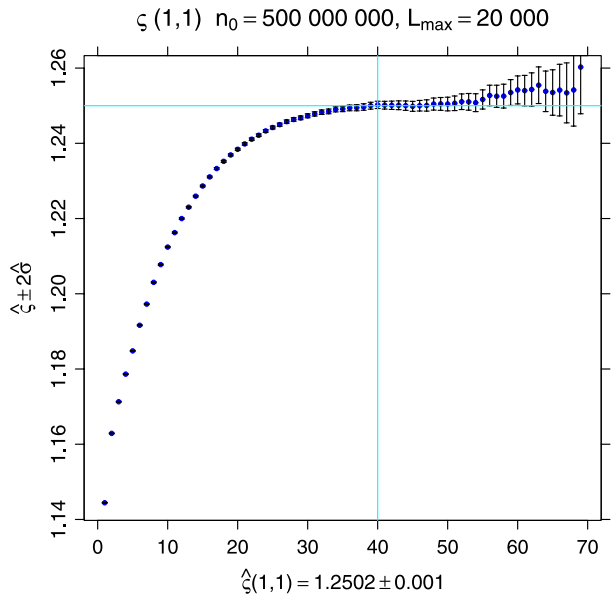


Fig. 3 Simulation for $\zeta_2(1, 1)$. The co-ordinate shows k_{\min} , the ordinate shows the corresponding $\hat{\zeta}$ with error bars. The vertical line indicates $k_{\min} = 40$ which we chose for our estimate of $\hat{\zeta}$. The horizontal line shows the true value



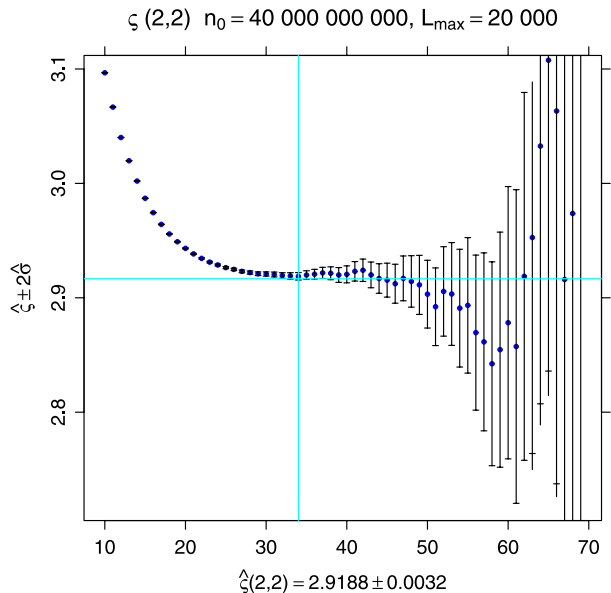
3.4.2 Exponent $\zeta(2, 2)$

The exact value $\zeta_2(2, 2) = 35/12 = 2.91666\dots$ is known. Also this simulation serves as a benchmark for our simulations.

L_k	n_k	L_k	n_k	L_k	n_k	L_k	n_k	L_k	n_k
30	40 000 000 000	113	459 313 243	455	7 559 087	1890	117 893	7881	1872
33	27 956 276 949	124	347 384 944	500	5 737 717	2079	89 442	8669	1450
36	19 934 507 109	136	263 528 000	550	4 343 548	2286	67 757	9535	1108
39	14 769 670 878	149	200 799 711	605	3 288 311	2514	51 314	10 488	853
42	11 270 896 745	163	153 819 037	665	2 496 057	2765	38 803	11 536	650
46	8 156 016 609	179	116 600 065	731	1 893 876	3041	29 341	12 689	479
50	6 108 280 379	196	89 210 485	804	1 434 709	3345	22 363	13 957	348
55	4 423 365 460	215	67 932 955	884	1 087 314	3679	16 949	15 352	266
60	3 315 611 015	236	51 656 232	972	823 685	4046	12 813	16 887	193
66	2 432 628 801	259	39 313 221	1069	624 023	4450	9738	18 575	151
72	1 842 369 408	284	30 007 400	1175	473 832	4895	7339	20 000	123
79	1 375 726 309	312	22 780 638	1292	359 121	5384	5571		
86	1 056 545 535	343	17 265 563	1421	271 557	5922	4218		
94	803 537 797	377	13 094 893	1563	205 432	6514	3229		
103	607 993 657	414	9 961 095	1719	155 585	7 165	2477		

Values used for the fit: $L_k = 605 \dots 20000$. CPU time 1879 h.

Fig. 4 Simulation for $\zeta_2(2, 2)$. The co-ordinate shows k_{\min} , the ordinate shows the corresponding $\hat{\zeta}$ with error bars. The vertical line indicates $k_{\min} = 34$ which we chose for our estimate of $\hat{\zeta}$. The horizontal line shows the true value



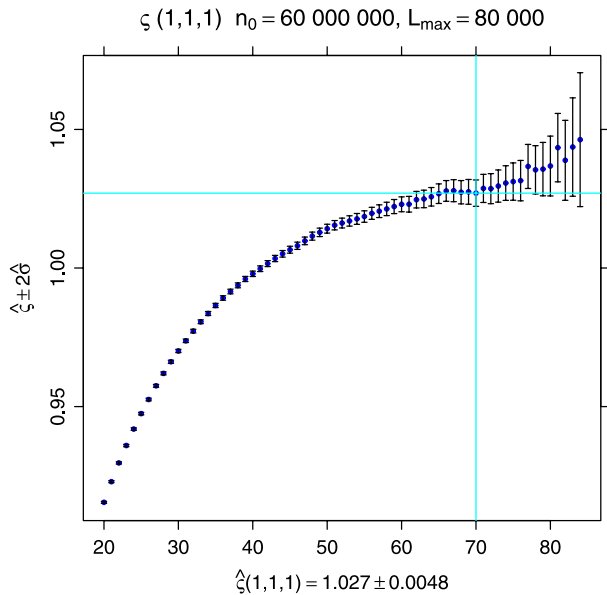
3.4.3 Exponent $\zeta_3(1, 1, 1)$

The exact value of $\zeta_3(1, 1, 1)$ is unknown.

L_k	n_k	L_k	n_k	L_k	n_k	L_k	n_k	L_k	n_k
30	60 000 000	149	25 859 377	804	5 614 962	4450	1 028 587	24 722	179 046
33	59 710 616	163	24 028 791	884	5 121 770	4895	934 379	27 194	162 421
36	58 947 709	179	22 226 328	972	4 670 981	5384	848 491	29 913	147 273
39	57 896 946	196	20 584 233	1069	4 256 241	5922	770 449	32 904	133 514
42	56 673 833	215	19 009 323	1175	3 879 722	6514	699 523	36 194	121 333
46	54 898 618	236	17 526 913	1292	3 534 606	7165	635 064	39 813	109 856
50	53 061 195	259	16 147 690	1421	3 218 775	7881	576 119	43 794	99 544
55	50 777 396	284	14 873 454	1563	2 930 010	8669	523 319	48 173	90 226
60	48 570 208	312	13 666 336	1719	2 666 485	9535	474 777	52 990	81 910
66	46 070 175	343	12 537 025	1890	2 426 899	10 488	430 885	58 289	74 069
72	43 747 356	377	11 494 795	2079	2 208 165	11 536	391 134	64 117	67 148
79	41 266 693	414	10 540 910	2286	2 009 516	12 689	354 964	70 528	60 809
86	39 014 779	455	9 652 748	2514	1 827 541	13 957	321 882	77 580	54 981
94	36 696 389	500	8 835 893	2765	1 661 614	15 352	291 736	80 000	53 301
103	34 372 986	550	8 076 259	3041	1 510 468	16 887	264 553		
113	32 097 711	605	7 376 857	3345	1 372 149	18 575	239 803		
124	29 906 035	665	6 740 503	3679	1 246 493	20 432	217 707		
136	27 820 941	731	6 155 608	4046	1 132 343	22 475	197 364		

Values used for the fit: $L_k = 18575 \dots 80000$. CPU time 8262 h.

Fig. 5 Simulation for $\zeta_3(1, 1, 1)$. The co-ordinate shows k_{\min} , the ordinate shows the corresponding $\hat{\zeta}$ with error bars. The vertical line indicates $k_{\min} = 70$ which we chose for our estimate of $\hat{\zeta}$. The horizontal line shows the estimated value



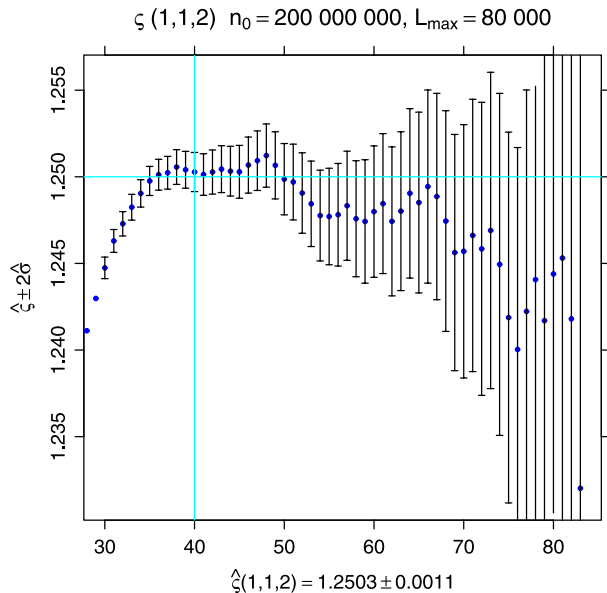
3.4.4 Exponent $\zeta_3(1, 1, 2)$

The exact value of $\zeta_3(1, 1, 2)$ is unknown.

L_k	n_k	L_k	n_k	L_k	n_k	L_k	n_k	L_k	n_k
30	200 000 000	149	54 585 738	804	7 029 965	4450	826 443	24 722	97 235
33	198 136 199	163	49 210 675	884	6 245 336	4895	733 837	27 194	86 246
36	193 436 538	179	44 119 702	972	5 545 792	5384	651 874	29 913	76 472
39	187 242 650	196	39 647 836	1069	4 923 405	5922	578 486	32 904	67 873
42	180 308 394	215	35 523 866	1175	4 374 033	6514	513 593	36 194	60 371
46	170 682 110	236	31 776 899	1292	3 885 012	7165	456 239	39 813	53 674
50	161 176 218	259	28 415 711	1421	3 449 618	7881	405 240	43 794	47 628
55	149 901 066	284	25 417 521	1563	3 062 025	8669	359 523	48 173	42 353
60	139 521 065	312	22 668 175	1719	2 718 548	9535	319 391	52 990	37 627
66	128 301 060	343	20 191 522	1890	2 415 286	10488	28 3792	58 289	33 387
72	118 361 321	377	17 981 958	2079	2 144 282	11 536	251 871	64 117	29 608
79	108 205 442	414	16 028 002	2286	1 904 636	12 689	223 767	70 528	26 339
86	993 85 254	455	14 267 282	2514	1 690 316	13 957	198 585	77 580	23 407
94	90 671 582	500	12 694 594	2765	1 499 756	15 352	176 146	80 000	22 541
103	82 304 628	550	11 279 842	3041	1 331 441	16 887	156 219		
113	74 445 095	605	10 020 648	3345	1 181 425	18 575	138 744		
124	67 187 208	665	8 909 164	3679	1 048 523	20 432	123 285		
136	60 566 796	731	7 917 614	4046	930 691	22 475	109 424		

Values used for the fit: $L_k = 1069 \dots 10\,000$. CPU time 5858 h.

Fig. 6 Simulation for $\zeta_3(1, 1, 2)$. The co-ordinate shows k_{\min} , the ordinate shows the corresponding $\hat{\zeta}$ with error bars. The vertical line indicates $k_{\min} = 40$ which we chose for our estimate of $\hat{\zeta}$. The horizontal line shows the conjectured value $\zeta_3(1, 1, 2) = \zeta_2(1, 1) = 5/4$



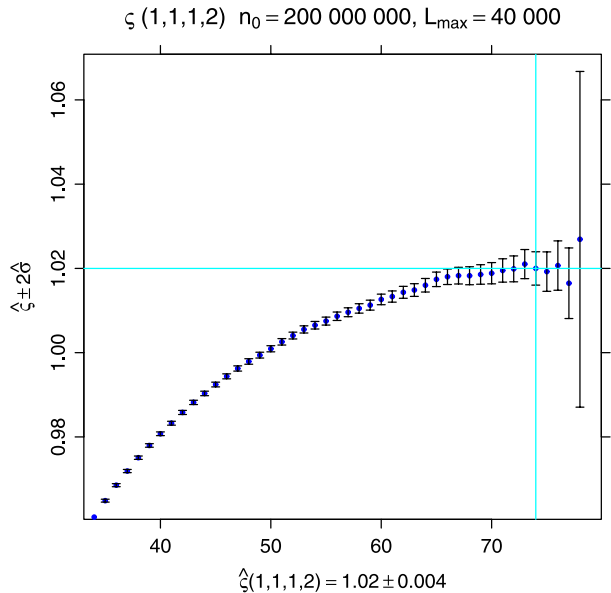
3.4.5 Exponent $\zeta_4(1, 1, 1, 2)$

The exact value of $\zeta_4(1, 1, 1, 2)$ is unknown.

L_k	n_k	L_k	n_k	L_k	n_k	L_k	n_k	L_k	n_k
30	200 000 000	124	126 992 806	550	38 132 997	2514	8 950 110	11 536	1 953 289
33	199 921 620	136	119 464 557	605	34 954 676	2765	8 149 013	12 689	1 773 558
36	199 482 984	149	112 181 604	665	32 040 238	3041	7 419 539	13 957	1 609 927
39	198 565 228	163	105 219 661	731	29 348 812	3345	6 752 347	15 352	1 461 067
42	197 176 986	179	98 203 442	804	26 850 724	3679	6 144 676	16 887	1 326 172
46	194 683 952	196	91 672 706	884	24 560 465	4046	5 589 138	18 575	1 203 707
50	191 624 492	215	85 304 312	972	22 451 887	4450	5 082 774	20 432	1 092 672
55	187 237 710	236	79 199 999	1069	20 511 329	4895	4 621 823	22 475	991 657
60	182 471 375	259	73 434 697	1175	18 739 197	5384	4 201 858	24 722	900 187
66	176 514 402	284	68 044 645	1292	17 110 256	5922	3 819 442	27 194	816 464
72	170 515 344	312	62 863 201	1421	15 612 645	6514	3 470 994	29 913	740 704
79	163 642 608	343	57 973 159	1563	14 238 301	7165	3 155 561	32 904	672 302
86	157 023 575	377	53 412 940	1719	12 983 348	7881	2 866 913	36 194	609 756
94	149 860 203	414	49 196 512	1890	11 838 167	8669	2 604 947	39 813	553 485
103	142 343 356	455	45 240 841	2079	10 786 022	9535	2 366 048	40 000	550 828
113	134 666 159	500	41 572 496	2286	9 827 571	10 488	2 149 715		

Values used for the fit: $L_k = 27 194, \dots, 40 000$. CPU time 35 212 h.

Fig. 7 Simulation for $\zeta_4(1, 1, 1, 2)$. The co-ordinate shows k_{\min} , the ordinate shows the corresponding $\hat{\zeta}$ with error bars. The vertical line indicates $k_{\min} = 74$ which we chose for our estimate of $\hat{\zeta}$. The horizontal line shows the estimated value



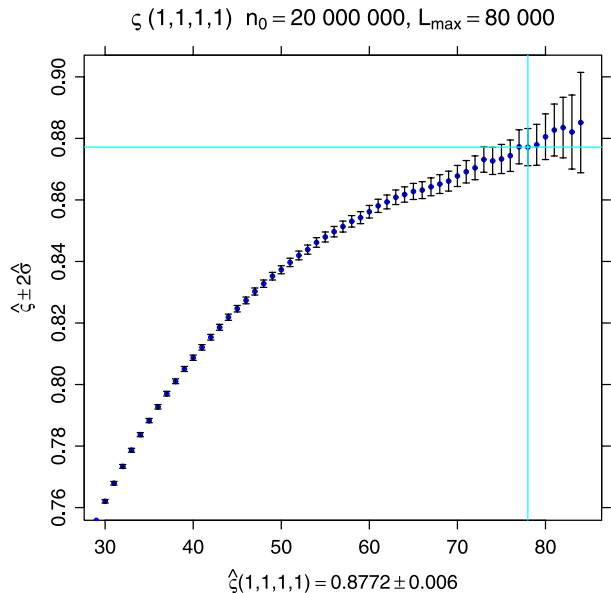
3.4.6 Exponent $\zeta_4(1, 1, 1, 1)$

The exact value of $\zeta_4(1, 1, 1, 1)$ is unknown.

L_k	n_k	L_k	n_k	L_k	n_k	L_k	n_k	L_k	n_k
30	20 000 000	149	13 677 483	804	4 613 179	4450	1 191 616	24 722	278 878
33	19 996 035	163	13 066 040	884	4 297 577	4895	1 101 052	27 194	256 535
36	19 972 855	179	12 433 477	972	4 001 670	5384	1 017 194	29 913	236 157
39	19 923 361	196	11 828 110	1069	3 722 426	5922	939 586	32 904	217 434
42	19 846 358	215	11 220 785	1175	3 461 745	6514	867 259	36 194	200 369
46	19 704 559	236	10 622 843	1292	3 217 081	7165	801 006	39 813	184 289
50	19 524 417	259	10 040 743	1421	2 987 877	7881	739 646	43 794	169 567
55	19 258 012	284	9 483 483	1563	2 773 980	8669	682 392	48 173	156 118
60	18 958 581	312	8 935 078	1719	2 573 328	9535	629 677	52 990	143 655
66	18 573 948	343	8 402 393	1890	2 386 906	10 488	580 582	58 289	132 091
72	18 172 653	377	7 892 203	2079	2 213 006	11 536	535 316	64 117	121 391
79	17 698 995	414	7 410 458	2286	2 051 046	12 689	493 266	70 528	111 643
86	17 228 707	455	6 946 326	2514	1 899 964	13 957	454 757	77 580	102 601
94	16 704 112	500	6 504 855	2765	1 758 768	15 352	419 131	80 000	99 860
103	16 136 193	550	6 081 417	3041	1 628 269	16 887	386 266		
113	15 537 061	605	5 681 289	3345	1 506 688	18 575	356 146		
124	14 922 694	665	5 304 532	3679	1 393 480	20 432	328 229		
136	14 299 200	731	4 949 662	4046	1 289 159	22 475	302 420		

Values used for the fit: $L_k = 39 813 \dots 80 000$. CPU time 18 262 h.

Fig. 8 Simulation for $\zeta_4(1, 1, 1, 1)$. The co-ordinate shows k_{\min} , the ordinate shows the corresponding $\hat{\zeta}$ with error bars. The vertical line indicates $k_{\min} = 78$ which we chose for our estimate of $\hat{\zeta}$. The horizontal line shows the estimated value



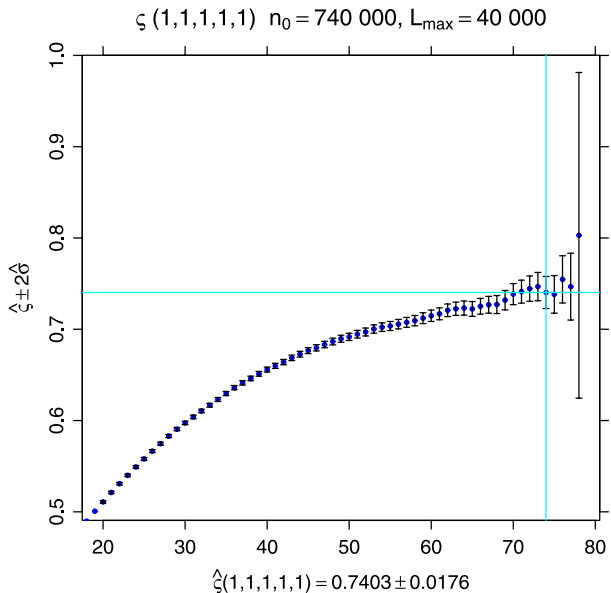
3.4.7 Exponent $\zeta_5(1, 1, 1, 1, 1)$

The exact value of $\zeta_5(1, 1, 1, 1, 1)$ is unknown.

L_k	n_k	L_k	n_k	L_k	n_k	L_k	n_k	L_k	n_k
30	744 165	124	663 493	550	370 165	2514	150 828	11 536	53 144
33	744 158	136	648 801	605	352 289	2765	141 592	12 689	49 724
36	744 107	149	633 473	665	335 283	3041	133 025	13 957	46 458
39	743 886	163	617 246	731	318 821	3345	124 845	15 352	43 355
42	743 487	179	599 664	804	302 365	3679	117 257	16 887	40 574
46	742 538	196	581 885	884	286 416	4046	109 961	18 575	37 983
50	741 155	215	562 961	972	271 268	4450	102 996	20 432	35 448
55	738 765	236	543 820	1069	256 593	4895	96 520	22 475	33 083
60	735 484	259	524 462	1175	242 487	5384	90 434	24 722	30 843
66	730 711	284	505 282	1292	229 014	5922	84 699	27 194	28 666
72	725 183	312	485 535	1421	216 285	6514	79 371	29 913	26 699
79	718 008	343	465 955	1563	204 002	7165	74 357	32 904	24 955
86	710 226	377	446 300	1719	192 310	7881	69 601	36 194	23 207
94	700 782	414	426 779	1890	181 055	8669	65 234	39 813	21 616
103	689 769	455	407 418	2079	170 456	9535	61 002	40 000	21 535
113	677 384	500	388 692	2286	160 399	10 488	56 977		

Values used for the fit: $L_k = 27 194 \dots 40 000$. CPU time 1147 h.

Fig. 9 Simulation for $\zeta_5(1, 1, 1, 1, 1)$. The co-ordinate shows k_{\min} , the ordinate shows the corresponding $\hat{\zeta}$ with error bars. The vertical line indicates $k_{\min} = 74$ which we chose for our estimate of $\hat{\zeta}$. The horizontal line shows the estimated value



3.4.8 Exponent $\zeta_3(1, 3, 3)$

The exact value of $\zeta_3(1, 3, 3)$ is unknown. As it turns out that $\zeta_3(1, 3, 3) > 2$, we have performed simulations according to our scheme 2. That is, we have generated n master samples of random walk paths that reach the boundary of the L_1 -box (here $L_1 = 10\,000$). For each such master sample i we have run $m = 1000$ trials and have counted the fraction \hat{p}_i of trials where the paths reached the boundary of the L_2 -box (with $L_2 = 2L_1$). As $n = 18\,100$ we cannot give the complete data set p_1, \dots, p_n but rather give the empirical mean and the standard deviation of \hat{p}

$$\hat{p} = 0.155202983425414, \quad \hat{\sigma}_p = 0.000536918044881792.$$

From this we compute

$$\hat{\zeta}_3(1, 3, 3) = 2.6877718045551$$

with standard deviation

$$\hat{\sigma} = 0.00499094143436367.$$

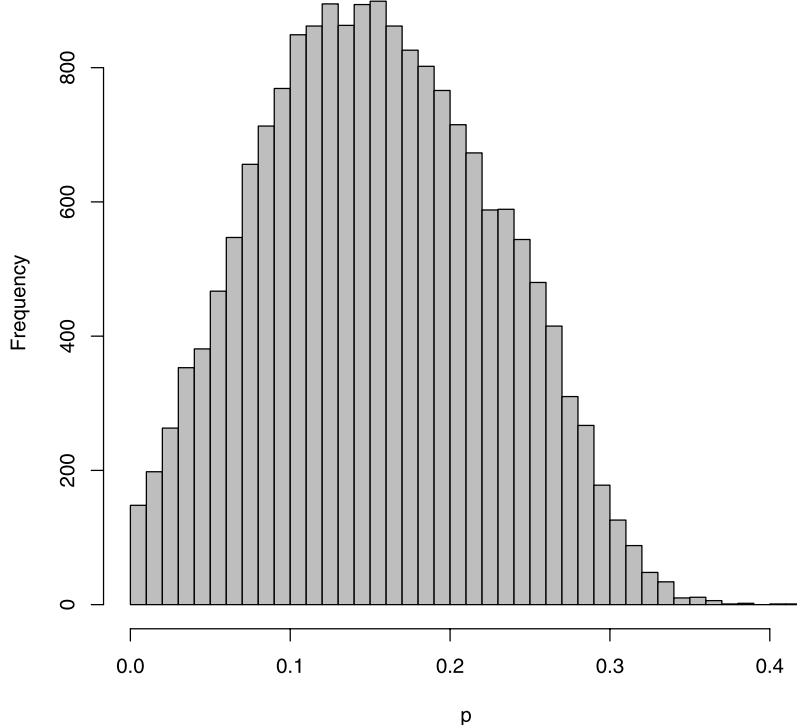
We conjecture that

$$\zeta_3(1, 3, 3) = \zeta_2(1, 3) = \frac{13 + \sqrt{73}}{8} = 2.693000\dots$$

We conclude with a histogram of the values p_i .

3.4.9 Exponent $\zeta_3(2, 2, 2)$

The exact value of $\zeta_3(2, 2, 2)$ is unknown. We have performed a simulation with the second scheme with $N = 16\,000$, $n = 1000$, $L_1 = 10\,000$, $L_2 = 20\,000$. Mean and standard

(1,3,3) Histogram of p , 18100 samples**Fig. 10** Histogram of the values p_i for $\xi_3(1, 3, 3)$

deviation are

$$\hat{p} = 0.1449495, \quad \hat{\sigma}_p = 0.000497221297799643.$$

From this we compute

$$\hat{\xi}_3(2, 2, 2) = 2.78637773802317$$

with standard deviation

$$\hat{\sigma} = 0.00494888703003405.$$

3.4.10 Exponent $\xi_3(2, 2, 3)$

The exact value of $\xi_3(2, 2, 3)$ is unknown. We conjecture

$$\xi_3(2, 2, 3) = \xi_2(2, 2) = \frac{35}{12} = 2.916666\dots$$

We have performed a simulation with the second scheme with $N = 23\,000$, $n = 1000$, $L_1 = 10\,000$, $L_2 = 20\,000$. Mean and standard deviation are

$$\hat{p} = 0.130559, \quad \hat{\sigma}_p = 0.00044444142417374.$$

From this we compute

$$\hat{\varsigma}_3(2, 2, 3) = 2.93722618256156$$

with standard deviation

$$\hat{\sigma} = 0.00491116935805033.$$

3.4.11 Exponent $\varsigma_3(2, 3, 3)$

The exact value of $\varsigma_3(2, 3, 3)$ is unknown. We conjecture

$$\varsigma_3(2, 3, 3) = \varsigma_2(2, 3) = \frac{47 + 5\sqrt{73}}{24} = 3.738334113 \dots$$

We have performed a simulation with the second scheme with $N = 1000$, $n = 1000$, $L_1 = 10000$, $L_2 = 20000$. Mean and standard deviation are

$$\hat{p} = 0.073458, \quad \hat{\sigma}_p = 0.00144828442088002.$$

From this we compute

$$\hat{\varsigma}_3(2, 3, 3) = 3.76693657262376$$

with standard deviation

$$\hat{\sigma} = 0.0284439101500224.$$

This simulation was particularly time consuming (179 543 h CPU time) as the actual value of $\varsigma_3(2, 3, 3)$ is rather large and it thus takes a tremendous amount of time to generate each master sample.

3.4.12 Exponent $\varsigma_4(2, 2, 2, 2)$

The exact value of $\varsigma_4(2, 2, 2, 2)$ is unknown. We have performed a simulation with the second scheme with $N = 16000$, $n = 1000$, $L_1 = 10000$, $L_2 = 20000$. Mean and standard deviation are

$$\hat{p} = 0.157732125, \quad \hat{\sigma}_p = 0.000521232849038418.$$

From this we compute

$$\hat{\varsigma}_4(2, 2, 2, 2) = 2.66445157389522$$

with standard deviation

$$\hat{\sigma} = 0.00476745017196814.$$

Acknowledgements P.M. is supported by the *Engineering and Physical Sciences Research Council (EPSRC)* through an Advanced Research Fellowship.

References

1. Burdzy, K., Lawler, G., Polaski, T.: On the critical exponent for random walk intersections. *J. Stat. Phys.* **56**, 1–12 (1989)
2. Camia, F., Newman, C.M.: Two-dimensional critical percolation: the full scaling limit. *Commun. Math. Phys.* **268**, 1–38 (2006)
3. Camia, F., Newman, C.M.: Critical percolation exploration path and SLE₆: a proof of convergence. *Probab. Theory Relat. Fields* **139**, 473–519 (2007)
4. Cardy, J.: Critical percolation in finite geometries. *J. Phys. A* **25**, L201–L206 (1992)
5. Duplantier, B.: Random walks and quantum gravity in two dimensions. *Phys. Rev. Lett.* **81**, 5489–5492 (1998)
6. Duplantier, B., Kwon, K.-H.: Conformal invariance and intersections of random walks. *Phys. Rev. Lett.* **61**, 2514–2517 (1988)
7. Duplantier, B., Sheffield, S.: Duality and the Knizhnik-Polyakov-Zamolodchikov relation in Liouville quantum gravity. *Phys. Rev. Lett.* **102**, 150603 (2009)
8. Klenke, A., Mörters, P.: The multifractal spectrum of Brownian intersection local time. *Ann. Probab.* **33**, 1255–1301 (2005)
9. Knuth, D.E.: *The Art of Computer Programming*, 3rd edn., vol. 2. Addison-Wesley, Boston (2005)
10. Lawler, G.F.: Intersections of random walks with random sets. *Isr. J. Math.* **65**, 113–132 (1989)
11. Lawler, G.F.: *Intersections of Random Walks*. Birkhäuser, Boston (1991)
12. Lawler, G.F.: Nonintersecting planar Brownian motions. *Math. Phys. Electron. J.* **1**, 1–35 (1995). Paper 4
13. Lawler, G.F.: Hausdorff dimension of cut points for Brownian motion. *Electron. J. Probab.* **1**, 1–20 (1996). Paper 2
14. Lawler, G.F., Schramm, O., Werner, W.: Values of Brownian intersection exponents I: Half-plane exponents. *Acta Math.* **187**, 237–273 (2001)
15. Lawler, G.F., Schramm, O., Werner, W.: Values of Brownian intersection exponents II: Plane exponents. *Acta Math.* **187**, 275–308 (2001)
16. Lawler, G.F., Schramm, O., Werner, W.: Values of Brownian intersection exponents III: Two-sided exponents. *Ann. Inst. Henri Poincaré* **38**, 109–123 (2002)
17. Lawler, G.F., Schramm, O., Werner, W.: Analyticity of intersection exponents for planar Brownian motion. *Acta Math.* **189**, 179–201 (2002)
18. Leath, P.L., Reich, G.R.: Scaling form for percolation cluster sizes and perimeters. *J. Phys. C* **11**, 4017–4036 (1978)
19. Lehmann, E.L.: *Theory of Point Estimation*. Wiley, New York (1983)
20. Li, B., Sokal, A.: High-precision Monte Carlo test of the conformal-invariance predictions for two-dimensional mutually avoiding walks. *J. Stat. Phys.* **61**, 723–748 (1990)
21. Mörters, P., Peres, Y.: *Brownian Motion*. Cambridge University Press, Cambridge (2009)
22. Mörters, P., Shieh, N.-R.: The exact packing measure of Brownian double points. *Probab. Theory Relat. Fields* **143**, 113–136 (2009)
23. Rhodes, R., Vargas, V.: KPZ formula for log-infinitely divisible multifractal random measures. [arXiv:0807.1036](https://arxiv.org/abs/0807.1036) (2008)
24. Saleur, B., Duplantier, B.: Exact determination of the percolation hull exponent in two dimensions. *Phys. Rev. Lett.* **58**, 2325–2328 (1987)
25. Smirnov, S.: Critical percolation in the plane: conformal invariance, Cardy’s formula, scaling limits. *C.R. Acad. Sci. Paris, Ser. I, Math.* **333**, 239–244 (2001)
26. Voss, R.F.: The fractal dimension of percolation cluster hulls. *J. Phys. A* **17**, L373–L377 (1984)